Arabian Journal of Geosciences (2022) 15: 1150
https://doi.org/10.1007/s12517-022-10420-y

ORIGINAL PAPER

Ichnology of the Cenomanian–Turonian boundary event in the southern Tethyan margin (Khanguet Grouz section, Ouled Nail Range, Algeria)

Mohammed Nadir Naimi[1] · Amine Cherif[1] · Chikh Younes Mahboubi[2] · Madani Benyoucef[3]

Received: 29 October 2021 / Accepted: 2 June 2022 / Published online: 10 June 2022

Abstract
The Cenomanian–Turonian boundary event (C/TBE) is studied in the southern Tethyan margin from an ichnological point of view for the first time. The ichnotaxa *Chondrites* isp., *Pilichnus* isp., *Planolites* isp., *Ptychoplasma* isp., *?Thalassinoides* isp. and *?Trichichnus* isp. are reported from the Cenomanian–Turonian succession of the Khanguet Grouz section (Ouled Nail Range, Algerian Saharan Atlas), subdivided into five informal units. The pre-event deposits are characterised by high abundance of burrows attributed to *Planolites* and *Ptychoplasma*, associated with bivalve and gastropod shells, which indicate that the ecological niche was occupied by different organisms with variable ethology. The beginning of the C/TBE is marked by an important change bioturbation intensity as well as ichnodiversity as revealed by the decrease of trace fossils, by either their generalised scarcity or their total absence. The recorded traces from the C/TBE deposits are *Chondrites*, *Pilichnus*, *Planolites*, *?Thalassinoides* and *?Trichichnus*, indicating stressful conditions, which is supported also by the joint presence of dwarfed forms of bivalves. The C/TBE black shales are laminated and largely unburrowed to sparsely burrowed, suggesting episodes of improved palaeoenvironmental conditions during which *Chondrites*, *Pilichnus* and *?Trichichnus* producers could colonise the substrate in unfavourable, dysoxic to anoxic benthic conditions. However, these black shales are intercalated by different facies characterising oxic conditions, as indicated by the presence of fauna (i.e. inoceramid bivalves). The post-event (or recovery) phase is characterised by high bioturbation intensity, with abundant *Planolites* and other undetermined burrows. As evidenced in the northern Tethyan margin, the important decrease in ichnoabundance and ichnodiversity is related to a significant decrease in the oxygenation of pore water. Moreover, the 'Oceanic Anoxic Event' ('OAE-2')-ichnoassemblage of the Khanguet Grouz section is similar to those found in the Rio Fardes section (Betic Cordillera, Spain), in comparison with the other Tethyan sections.

Keywords Trace fossils · Cenomanian–Turonian boundary event · Dysoxia · Black shales · Palaeoenvironments · Ouled Nail Range · South Tethyan realm

Introduction

The Cenomanian–Turonian boundary (C/TB = 93.9 Ma; Gradstein et al. 2012) interval containing the black shales of the Oceanic Anoxic Event 2 (OAE-2) records major

Responsible Editor: Attila Ciner

✉ Mohammed Nadir Naimi
naimi.mohamed_nadir@univ-ouargla.dz

Amine Cherif
acherif11@gmail.com

Chikh Younes Mahboubi
mahboubi_32@hotmail.com

Madani Benyoucef
benyoucefmada@gmail.com

[1] Laboratoire de Géologie du Sahara, Université Kasdi Merbah Ouargla, Route de Ghardaïa BP. 511, 30000 Ouargla, Algeria

[2] Département Des Sciences de La Terre, FSTU, Université Mohamed Ben Ahmed, Oran 2, 1524 El M'naouer, 31000 Oran, Algeria

[3] Faculty of Natural and Life Sciences, University Mustapha Stambouli of Mascara, 29000 Mascara, Algeria

oceanographic change in the marine environment (e.g. Arthur et al. 1988), as well as the highest Mesozoic–Cenozoic sea level stand (Haq et al. 1987). It is characterised by the Cenomanian–Turonian boundary event (C/TBE) which is considered one of the major Mesozoic events (2–3‰ positive $\delta^{13}C$ excursion) (Scholle and Arthur 1980). This event is related to widespread oceanic anoxia described asOAE-2 (Schlanger and Jenkyns 1976), enhanced rates of organic carbon burial, major faunal change and demise of tropical carbonate platforms. This period was also a turning point in marine radiation and extinction of many macrofossil and microfossil groups (e.g. Hallam and Wignall 1997). The productivity event of the OAE-2 had a major effect on the calcareous nannoplankton and radiolarians (Leckie et al. 2002). Additionally, the OAE-2 affected deeper-dwelling planktonic foraminifera as evidenced by the extinction of the genus *Rotalipora* (e.g. Hart 1980; Wonders 1980).

This event is well documented in the Mediterranean area and surrounding margins. In Algeria, it has been evidenced geochemically, using total organic carbon (TOC) and stable isotope ($\delta^{13}C$ and $\delta^{18}O$) studies, and micropalaeontologically, on the basis of foraminifera and ostracods, in the Ouled Nail, Tebessa Ranges and Aures Mountains (Grosheny et al. 2008; Ruault-Djerrab and Kechid-Benkherouf 2011; Ruault-Djerrab et al. 2012, 2014; Salmi-Laouar et al. 2018). In the Ksour Range, the organic-rich facies (i.e. black shales) are absent, but the presence of a positive excursion zone of the $\delta^{13}C$ around the C/TB allowed evidencing the C/TBE (Salhi et al. 2020). This event coincides with the successive proliferation of different opportunistic organisms such as small gastropods and echinoids (Benadla et al. 2018). Further to the north, in the Ouarsenis Range, Benhamou and Brahim (2020) discovered a rich ichthyofauna in the Upper Cenomanian, organic-rich and siliceous deposits indicating the C/TBE. Furthermore, in the Tinrhert intracratonic basin (eastern Algerian Sahara), the study of the stratigraphic evolution of the ostracofauna suggested the presence of several bioevents related to the OAE-2 (Tchenar et al. 2020).

In the last few decades, many Phanerozoic mass-extinction events (i.e. oceanic anoxic events) were studied from an ichnological point of view, such as the Frasnian–Famennian boundary interval (Kellwasser Event, Stachacz et al. 2017), the end-Permian mass extinction (EPME, Rodríguez-Tovar et al. 2021), the Toarcian Oceanic Anoxic Event (T-OAE, e.g. Miguez-Salas et al. 2017), the latest Hauterivian Faraoni event (Rodríguez-Tovar and Uchman 2017), the Cretaceous–Paleogene (K/Pg; previously K/T) boundary (Bayet-Goll et al. 2014; Łaska et al. 2017) and the Paleocene–Eocene thermal maximum (PETM, Rodríguez-Tovar et al. 2011). Several works have addressed the ichnology of the C/TBE in the northern margin of the Tethys in order to obtain information on the response of the macrobenthonic trace maker communities, especially in Poland (e.g. Uchman et al. 2008, 2013a, b), Spain (Rodríguez-Tovar et al. 2009a, b, 2020), Italy (Monaco et al. 2012, 2016) and France (Olivero and Gaillard 1996). However, the C/TBE of the southern margin of the Tethyan realm has never been studied so far from an ichnologic standpoint.

Despite the numerous works addressed to the geochemistry and the micropalaeontology of the C/TBE from the different Algerian basins (Grosheny et al. 2008; Ruault-Djerrab and Kechid-Benkherouf 2011; Ruault-Djerrab et al. 2012, 2014; Salmi-Laouar et al. 2018; Benadla et al. 2018; Tchenar et al. 2020), its ichnological content has never been studied. This paper aims to (i) report trace fossils from the C/TBE of the southern Tethyan margin for the first time; (ii) describe the succession in order to interpret the evolution of palaeoenvironment; and (iii) discuss the palaeoecology and the response of the benthic communities to the anoxic event.

Geological setting

The studied section is located in the northwestern part of the Khanguet Grouz sub-circular structure. The latter corresponds to an anticline pertaining to the Ouled Nail Range, in the eastern part of the Saharan Atlas (Fig. 1A). Kazi-Tani (1986) integrated this anticline in the Slim synclinorium.

The Saharan Atlas is an intra-continental fold belt, oriented NE-SW. It forms the southwestern part of the Algerian Atlasic domain, which comprises also of the Aures Range, Zibane Mountains, Nementcha-Tebessa Range and Negrine Mountains, as well as the Oran Meseta and the Tlemcen domain. The latter constitute, together with the Tell Atlas, the Algerian part of the Alpine Mediterranean chain. This fold belt is composed of Mesozoic–Cenozoic shallow marine and continental deposits, uplifted during the Atlasic tectorogenic phase or the Atlas event, which is attributed to the Bartonian–Priabonian (late Eocene) and characterised by NE-SW to ENE-WSW trending folds (Guiraud 1973). The Saharan Atlas is subdivided into three segments: (i) the Ksour Range in the southwest, (ii) the Amour Range in the central part and (iii) the Ouled Nail Range in the north-east (Ritter 1902; Naimi et al. 2021a).

In the Ouled Nail Range, the oldest strata, attributed to the Triassic, are outcropping in complex faulted and diapiric zones (e.g. Aïn Ograb and Mgabret Zerigat) (Fig. 1B). They consist of purplish clays, gypsum, dolostones and dolerites (Emberger 1960). Due to their evaporitic nature, which is easily weathered and eroded, these diapirs have a low relief (Djebbar 2000). The Lower Cretaceous strata are represented by (i) Valanginian–Hauterivian marine deposits, (ii) Barremian and Lower Aptian continental (Bedoulian) and lagoonal plant-bearing sandstones showing rare dolomitic intercalations, (iii) Upper Aptian (Gargasian) carbonate deposits with abundant and diversified fauna and flora,

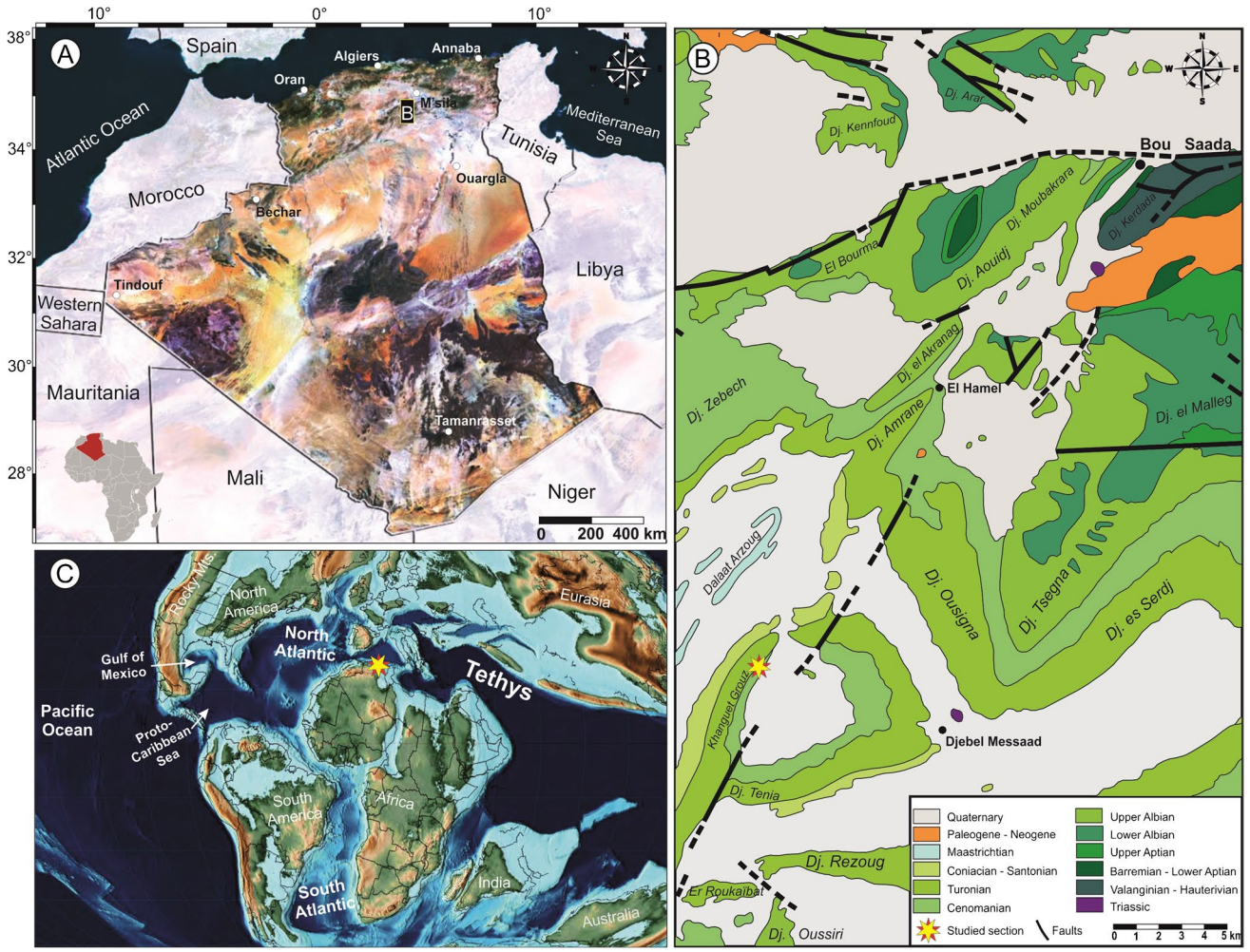

Fig. 1 Geological setting. **A** Satellite image showing the main geological characteristics of Algeria. **B** Simplified geological map of the Bou Saada area (modified after the geological map of Bou Saada 1/200,000). **C** Late Cenomanian global palaeogeography and location of the Ouled Nail basin (map after Scotese 2014)

(iv) Lower Albian deltaic and continental detrital deposits and (v) Upper Albian shallow marine oyster-rich carbonate deposits (e.g. Emberger 1960; Naimi and Cherif 2021; Naimi et al. 2021b). The lithofacies and bio facies of the lower Cenomanian are similar to those of the Upper Albian. They are overlain by Middle Cenomanian marl-limestone alternations and thick gypsum levels indicating a lagoonal environment, intercalated by some limestone beds rich in foraminifera (Emberger 1960). The upper part of the Cenomanian series is characterised by micritic, nodular and shelly limestones and black shales of the OAE-2 (Grosheny et al. 2008). During this period, the studied area constituted a part of the southern Tethyan margin (Benyoucef et al. 2017) (Fig. 1C).

Turonian deposits are represented by micritic limestones containing ammonites, inoceramids and planktonic foraminifera. In the Late Turonian, the environment becomes very shallow, characterised by echinoid-rich and oyster-rich marls and ooidal limestones with debris of rudists and corals (Emberger 1960). The post-Turonian Cretaceous displays the same features as the underlying Turonian deposits, while Coniacian–Santonian strata are represented by marls and gypsum at their base and foraminifer-bearing limestones at their top, whereas the overlying Campanian is highly fossiliferous and entirely marly. Furthermore, the Maastrichtian is characterised by chalky, dolomitic and ooidal, sub-reefal limestones. The Cenozoic strata lie unconformably on the Cretaceous deposits and are represented mainly by continental detrital deposits, such as conglomerates and sandy clays (Emberger 1960).

In the Khanguet Grouz, Herkat (1999) subdivided the Cenomanian–Turonian interval into two megasequences which characterise all the eastern part of the Algerian Atlasic domain: (i) Vraconnian–Cenomanian and (ii) Turonian. Only the upper part of the first one can be observed in the Khanguet Grouz section. However, the second one

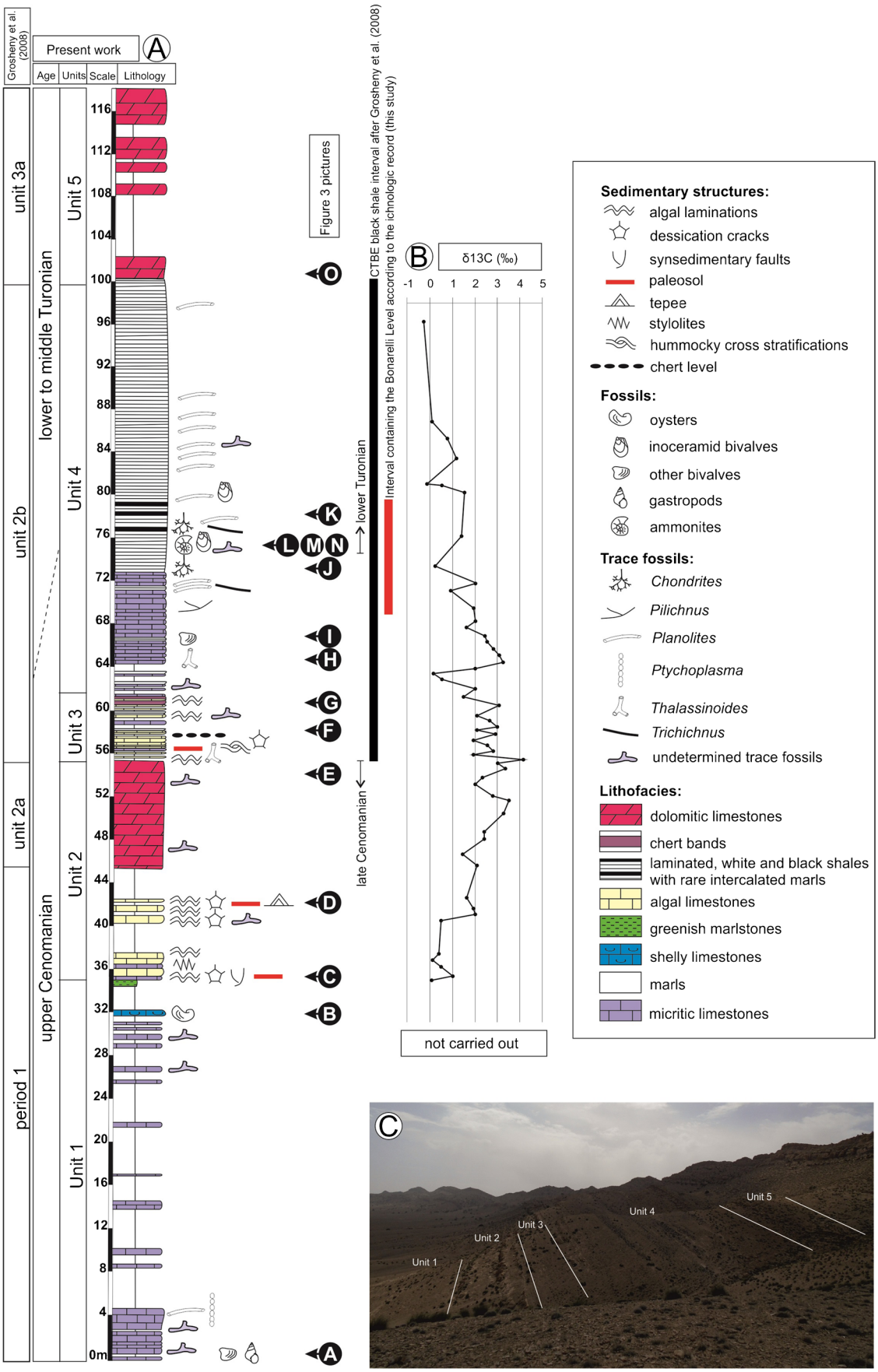
Grosheny et al. (2008)
Present work
A
Age
Units
Scale
Lithology
period 1
unit 2a
unit 2b
unit 3a
upper Cenomanian
lower to middle Turonian
Unit 1
Unit 2
Unit 3
Unit 4
Unit 5
116
112
108
104
100
96
92
88
84
80
76
72
68
64
60
56
52
48
44
40
36
32
28
24
20
16
12
8
4
0m
Figure 3 pictures
O
K
L
M
N
J
I
H
G
F
E
D
C
B
A
late Cenomanian
lower Turonian
Interval containing the Bonarelli Level according to the ichnologic record (this study)
CTBE black shale interval after Grosheny et al. (2008)
B
δ13C (‰)
-1
0
1
2
3
4
5
not carried out
Sedimentary structures:
algal laminations
dessication cracks
synsedimentary faults
paleosol
tepee
stylolites
hummocky cross stratifications
chert level
Fossils:
oysters
inoceramid bivalves
other bivalves
gastropods
ammonites
Trace fossils:
Chondrites
Pilichnus
Planolites
Ptychoplasma
Thalassinoides
Trichichnus
undetermined trace fossils
Lithofacies:
dolomitic limestones
chert bands
laminated, white and black shales with rare intercalated marls
algal limestones
greenish marlstones
shelly limestones
marls
micritic limestones
C
Unit 1
Unit 2
Unit 3
Unit 4
Unit 5

◂**Fig. 2** Lithostratigraphic succession of the Khanguet Grouz section. **A** Stratigraphic column of the Khanguet Grouz section. **B** Carbone isotope data (Grosheny et al. 2008). **C** Panoramic view of the studied succession

is well represented, which constitutes their type section for the Ouled Nail basin axis, composed of three 4th-order sequences and six 3rd-order sequences. Three periods were distinguished prior to and after the C/TBE in the same part of the Algerian Atlasic domain (Grosheny et al. 2008; Chikhi-Aouimeur et al. 2011).

The sub-circular structure of Khanguet Grouz is 7.5 km in diameter, represented by Cenomanian, Turonian and Coniacian–Santonian carbonate deposits. The younger strata (Turonian and Coniacian–Santonian) form prominent ridges around this structure such as Djebel Tenia in the southern part of the structure (Fig. 1B). To the east of the structure, a Triassic diapir evidenced by salt deposits crops out near the Aïn Ograb village (Djebel Messaad; Fig. 1B). Herkat (1999) interpreted this structure as resulting from a rotational deformation phase, due to the dextral shear of the North Atlas Fault. However, Djebbar (2000) mapped three main radial faults across the Khanguet Grouz structure, and assumed that this structure is likely to be the result of the salt diapir. The El Medaouar sub-circular structure, which is 3.2 km in diameter, located about 10 km to the west of the Khanguet Grouz structure and closely resembling the latter, has been attributed to a compressional event (rotational motion), corresponding to that of the Atlasic phase, which occurred during the Bartonian–Priabonian transition (~ 35 Ma) (Hassani et al. 2016). On the other hand, Kazi-Tani (1986) indicated that the circular folds of the Algerian Atlasic domain must be related to two different tectonic phases.

Methodology

The Khanguet Grouz section (ca. 35° 01′ 24″ N 3° 58′ 55 ″ E) is located in the Wilaya of M'sila (northern Algeria), near the road linking the RN46 to the RN89 (RN = national road), about 20 km southwest of Bou Saada town (Fig. 1B). The fieldwork had been carried out in April 2021 by the two first authors. The section was sampled, described bed-by-bed and subdivided into five informal units based on their lithological change, geometry, colour, trace fossils, sedimentary structures and faunal content. The facies and invertebrate fossils (bivalves, gastropods and ammonites) were photographed in situ. Trace fossils were mainly studied in the field and ichnotaxonomic analysis was complemented with photographs and collected specimens. They were systematically studied bed-by-bed, paying special attention to their distribution along the section, their abundance and their relationship within the different facies. Ichnological analysis involved the identification and recognition of trace fossils (Knaust 2012a), degree of bioturbation or bioturbation index (BI) (Taylor and Goldring 1993), as well as abundance and distribution of ichnotaxa (Knaust 2012b). The main macroscopic features used in the description of the recorded traces are shape of burrow, orientation, diameter, length and width. The toponomy of each trace fossil was recorded using Martinsson's classification (Martinsson 1970). The studied trace fossils were photographed in situ and they were not collected. Also, they have been arranged in alphabetical order.

Lithostratigraphy

At the Khanguet Grouz sub-circular structure, the Cenomanian–Turonian succession is subdivided into five informal units on the basis of detailed lithologic, sedimentologic, palaeontologic and ichnologic characteristics (Fig. 2).

Unit 1

This 35-m-thick unit starts with micritic limestones (0.2–0.5 m) containing many shells of bivalves and gastropods, intercalated by some marly levels (0.1–0.4 m). These latter are capped by a laminated limestone bed (0.4 m) (Fig. 3A), a marly level (0.3 m) and a bed of yellowish micritic limestones (1.6 m), grey in cross section and highly bioturbated at the base with abundant *Planolites* and *Ptychoplasma*. The intensity of bioturbation (BI) according to Taylor and Goldring (1993) is 4. The middle part of this unit (~ 25 m) is hidden along the circular structure by recent eluvial deposits, but some limestone beds crop out. The upper part is represented by bioturbated micritic limestone (0.2–0.4 m) and whitish marl (0.2–0.5 m) alternations. They are overlain by an oyster-rich limestone storm bed (0.3 m) and a whitish marl level (0.25 m). The oyster shells are fragmented and randomly oriented (Fig. 3B). This unit terminated by greenish laminated marlstones (0.6 m) is intercalated by some limestone levels.

Unit 2

The lowermost base of this 21-m-thick unit comprises a Lofer cyclothem constituted at its base by whitish limestones (0.3 m), overlain by yellowish stromatolitic limestones (0.6 m), containing loferitic breccias and affected by synsedimentary faults (growth faults) (Fig. 3C). Stromatolites exhibit both repetitive and alternating lamination. These stromatolitic limestones are sometimes marmorised. They are capped by a continuous micritic limestone bed (0.4 m), showing abundant bed-parallel horizontal to sub-horizontal stylolites, and resembling the member C of the typical Lofer cyclothems, thin limestones with algal laminations (0.8 m),

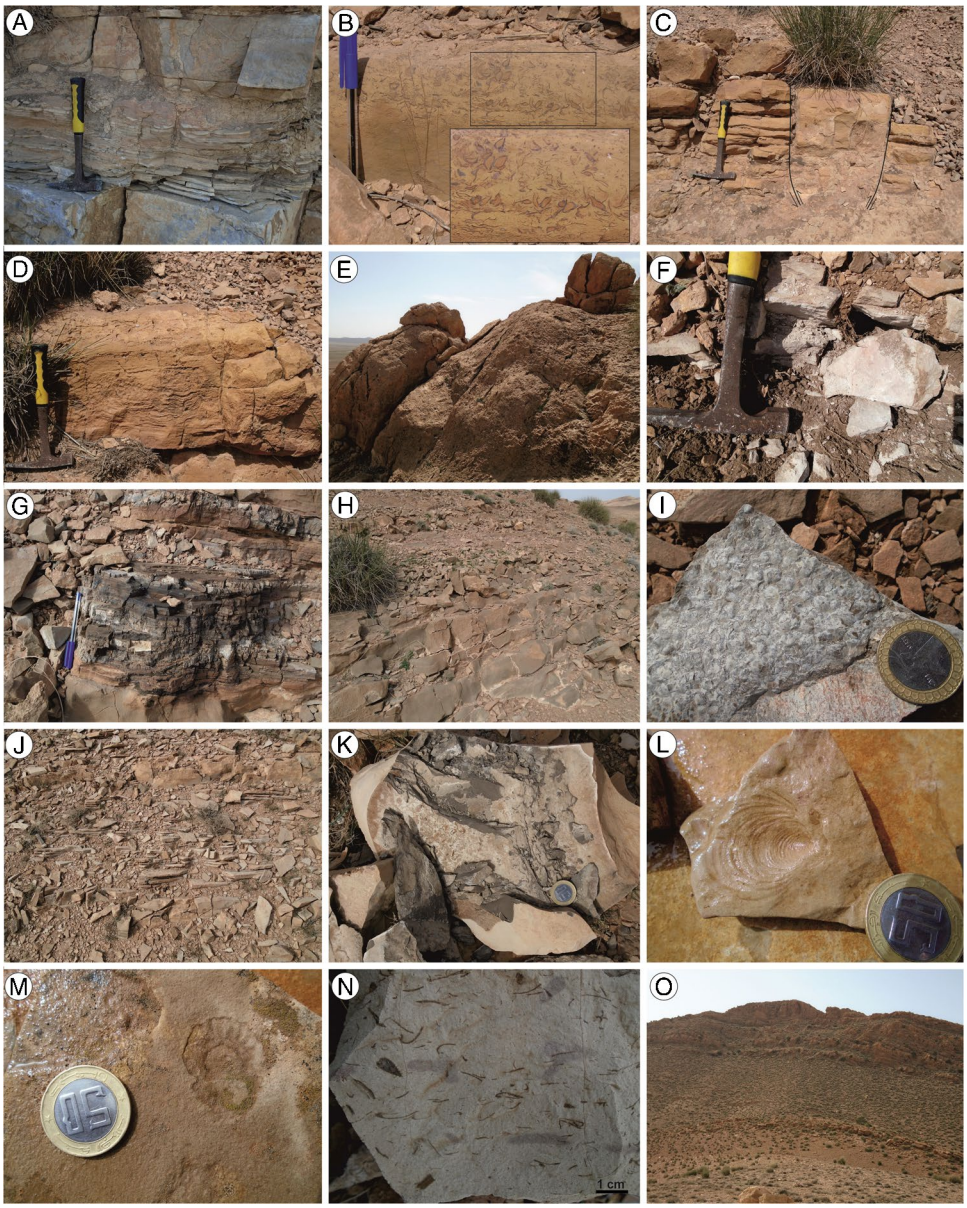

Fig. 3 Field photographs of the measured stratigraphic section. **A** Laminated limestones of unit 1. **B** Oyster-rich limestone storm bed. **C** Syn-sedimentary fault. **D** Algal limestone bed showing tepee structures. **E** Bioturbated dolomitised limestone bar (unit 2a sensu Grosheny et al. 2008). **F** Whitish shales of unit 3. **G** Chert bed. **H** Greyish micritic limestones. **I** Dwarfed bivalves from whitish shales intercalated in the greyish micritic limestones. **J** Whitish shales of the deepening facies. **K** Laminated black shales intercalated in the whitish shales. **L** Inoceramid bivalve *Mytiloides goppelnensis*. **M** Crushed ammonite associated with inoceramid bivalves. **N** Highly bioturbated whitish shales with *Planolites* and *?Trichichnus* burrows as well as bioclasts of oysters. **O** Marl-dolomitised limestone alternations of the upper part of the section

and by whitish marls (2.5 m). These latter are overlain by stromatolitic yellowish limestones (0.5 m), with sharp erosive bases, tepee structures (Fig. 3D) and red palaeosols, a loferitic breccia (0.2 m), micritic greyish limestones (0.3 m), and by another whitish marl interval (0.4 m).

The upper part of this unit begins by laminated limestones showing a palaeosol and desiccation cracks, whitish marls (0.3 m) and a limestone bed (0.3 m) bounded by another palaeosol. On this latter, whitish marls (0.1–3 m) which alternate with some micritic limestones (1–1.5 m) crop out. All these deposits consist in the period 1 of Grosheny et al. (2008). These authors considered these deposits complex and organised into successive shallow-water marl-limestone parasequences, maybe bounded by emersion surfaces. They also indicated that similar deposits characterise equivalent strata along the northern edge of the Saharan craton, through the south of Tunisia. In the Djebel Chbeibita section located further to the northwest, the lower part of this bar yielded Radiolitid fragments (Grosheny et al. 2008).

The unit 2 terminates by a thick bar (~ 10 m) of bioturbated dolomitic limestones (Fig. 3E) which corresponds to unit 2a of Grosheny et al. (2008). It is attributed to the late Cenomanian thanks to the presence of the ammonites *Euomphaloceras costatum*, *Metengonoceras* gr. *dibbleyi* and *Neocardioceras* sp. at the top of this thick bed (Herkat 1999).

Unit 3

This 7.5-m-thick unit begins by alternations of fine micritic limestones showing rare algal laminations and whitish

laminated biodetrital limestones with clayey and marly intervals (0.05–0.3 m). The limestone beds are 0.1–0.3-m thick. A Lofer cyclothem was found in the lowermost part of this unit. It is formed at the base by micritic limestones (0.2 m) with rare bivalve bioclasts and *?Thalassinoides* burrows, overlain by a palaeosol (0.05 m), and finally by a loferitic breccia.

The upper part of this unit starts with whitish shales (0.1 m) (Fig. 3F), overlain by alternations of micritic limestones (0.35 m), algal limestones showing some chert levels (0.25 m) and whitish shales (0.35 m), with marl levels (0.2–0.4 m).

This unit ends up with alternations of marls (0.1–0.15 m) and pseudo-nodular limestones (0.2–0.25 m), followed by two chert beds (0.4–0.5 m) interbedded by yellowish limestones with algal laminations. The cherts are blackish or whitish, very hard, well-stratified to nodular (Fig. 3G). They are passing laterally into greyish micritic limestones with algal laminations and thin black chert levels.

This unit 3 corresponds to the lowermost part of unit 2b of Grosheny et al. (2008), considered a black shale interval, and attributed to the C/TB interval.

Unit 4

This 38-m-thick unit starts with four sequences composed of three lithofacies: whitish marls (0.15–1.2 m), bioturbated micritic limestones (0.2–0.9 m) and white shales (0.3 m). These latter are capped by 8 m of greyish micritic limestones (Fig. 3H) with *?Thalassinoides* at the base and *Pilichnus*, *Planolites* and *?Trichichnus* at the top, intercalated by some whitish, thin shale beds showing dwarf bivalves (Fig. 3I). The bioturbation index of these levels is of about 3. A deepening facies characterises the upper part of this unit. It is very thick (~ 28 m), composed of whitish shales (0.05–0.25 m) (Fig. 3J), with some marl and/or clay intercalations. Many black shale levels are also present (Fig. 3K). Both whitish and black shales are laminated. The recorded fauna from the upper part of this unit 4 is represented by abundant inoceramid bivalves assigned to *Mytiloides goppelnensis* (Fig. 3L), with several juvenile forms. Their ornamentation consists of commarginal and rounded rugae; it is well-preserved and very characteristic besides the juvenile specimens. This species indicates early Turonian age since it appears in the Turonian GSSP (Greenhorn Limestone, Bridge Creek Member) at Pueblo (Colorado, USA) shortly above the base of the stage (beds 90 to 114; Kennedy et al. 2005); it does not reach the top of the substage. *Mytiloides goppelnensis* previously recorded from North America (Colorado), Europe (England, France, Germany, Poland, Russia and Spain), Japan and Iran (Kennedy et al. 2000; Wilmsen et al. 2020). Subsequently, the studied specimens are considered to constitute the first record from Africa. At the Khanguet Grouz section, this inoceramid bivalve is associated with crushed ammonites (Fig. 3M). Grosheny et al. (2008) reported the ammonite *Mammites* sp. from these deposits, thus confirming the age attributed thanks to inoceramids. Salmi-Laouar et al. (2018) reported *Mytiloides* inoceramids from the Lower Turonian (15 m above the first occurrence of *Whiteinella praehelvetica*) of the Morsott-Hameimat-Tebessa basin, a part of the Atlas domain, located to the north-east of the eastern Saharan Atlas (Ouled Nail Range).

The white shales are moderately to highly bioturbated (BI = 3–4) with abundant *Planolites*, common *Chondrites* and rare *?Trichichnus*, which are filled with purplish material (Fig. 3N). Dwarf bivalve shells are present in this facies. Furthermore, several beds contain oyster fragments which are randomly oriented (Fig. 3N). The black shales are laminated, largely unburrowed (BI = 0) to sparsely burrowed (BI = 1) and devoid of any faunal content. This unit 4 corresponds to the upper part of unit 2b of Grosheny et al. (2008). These authors described this unit as black, laminated shales alternating with black mudstones.

Unit 5

It consists of unit 3a of Grosheny et al. (2008). It is represented at the base by spaced alternations which become narrower at the top, of whitish marls (0.1–6.2 m) and dolomitic limestones (0.4–2.4 m) (Fig. 3O). The overlaying deposits are characterised by Astartidae-rich beds interpreted as tempestites (Grosheny et al. 2008). Their upper part presents tepee structures as well as evaporite dissolution breccias (Grosheny et al. 2008). Equivalent strata from the Djebel Chbeibita section yielded the ammonite *Romaniceras* sp. just above the Astartidae-rich limestones, therefore leading to assign this unit to the Upper Turonian.

Previous carbon isotope study

In the Khanguet Grouz section, the $\delta^{13}C$ data have been published by Grosheny et al. (2008). The isotopic curve of 56 samples from carbonates bulk has shown major positive $\delta^{13}C$ excursion range from − 0.3 to + 4.2 ‰ (Fig. 2B). In this paper, we try to reinterpret the results in light of new data and new interpretations in geochemistry. Three trends have been observed:

The first trend of $\delta^{13}C_{carb}$ shows positive values from + 0.1 to + 4.2 ‰ with positive anomaly up to + 4.00 ‰; this trend occurs in shallow limestone-marls alternation and bioturbated dolomitic limestones during the Upper Cenomanian (unit 2). The second trend of $\delta^{13}C_{carb}$ shows a fall from + 4.2 to + 0.2 ‰ and change rapidly to positive anomaly up to + 3.3 ‰ occurs in the beginning of micritic

limestones during the Upper Cenomanian–Lower Turonian transition (unit 3—lowermost part of unit 4). The third trend is characterised by fluctuations of $\delta^{13}C_{carb}$ ranging between − 0.3 and + 3.1 ‰ and occurs in micritic limestones as well as the whitish shales during the ?Lower–Middle Turonian (most of unit 4).

Synopsis of trace fossils

We recognised six ichnotaxa preserved mainly as epichnia, hypichnia and endichnia: *Chondrites* isp., *Pilichnus* isp., *Planolites* isp., *Ptychoplasma* isp., ?*Thalassinoides* isp. and *?Trichichnus* isp. (Table 1). Their determination was problematic because of their very poor preservation due to diagenetic obliteration.

Chondrites isp. (Fig. 4A)

This trace fossil is observed in cross section as endichnial. It appears as patches of circular to elliptical spots or short strait to slightly curved branches, some 0.5–2.5-mm wide. These are cross sections of a branched-down tunnel system filled with purplish material different from the whitish host rock. *Chondrites* isp. occurs deeper than 10 mm below bed tops. It is associated with *Planolites* isp. and *?Trichichnus* isp. *Chondrites* comprises several named ichnospecies, e.g. *C. affinis*, *C. caespitosus*, *C. intricatus*, *C. patulus*, *C. recurvus*, *C. stellaris* and *C. targionii* (Fu 1991; Uchman 1999; Uchman et al. 2012). The smaller forms of the C/TB *Chondrites* (0.5–1.5 mm) may be assigned to *C. intricatus* and *C. stellaris*, whereas the largest ones (2–3 mm) are generally attributed to *C. targionii* (e.g. Uchman et al. 2008; Rodríguez-Tovar et al. 2009a, 2020). The ichnogenus *Chondrites* constitutes the most representative trace fossil of the OAE-2 (see Table 2). It has been reported from other organic-rich deposits such as the latest Hauterivian Faraoni event in Spain (Rodríguez-Tovar and Uchman 2017) and the Valanginian organic-rich strata of the Ouarsenis Range in northwestern Algeria (Cherif et al. 2021a). This trace fossil occurs from near-shore storm beds to deep-sea muddy deposits and turbidites (Uchman et al. 2003; Cherif et al. 2015, 2021a; Bayet-Goll et al. 2017, 2020; Nasiri et al. 2020; Sharafi et al. 2022). The *Chondrites* burrow is built in order to obtain food, and is considered a fodinichnion of worm-like organisms, an agrichnion of asymbiotic bivalves, or a chemichnion of chemosymbiotic bivalves (Baucon et al. 2020). Furthermore, it could suggest very low oxygen conditions and represents a good indicator of dysoxic settings (Bromley and Ekdale 1984; Knaust 2017). The tracemakers of *Chondrites* may be able to live chemosymbiotically at the oxic/anoxic interface (Seilacher 1990; Fu 1991). This trace fossil can be present also in oxygenated seawater conditions (e.g. Belaid et al. 2020; Cherif and Naimi 2022; Cherif et al. 2021b).

Pilichnus isp. (Fig. 4B)

It consists of epichnial, small, narrow, horizontal, tabular and slightly winding grooves, showing *Y*-shaped dichotomous branches. Angles of branches reach 45°. *Pilichnus* isp. is less than 0.5-mm wide, and 0.8–27-mm long. It is filled by a lighter-coloured material than that of the host rock. The ichnogenus *Pilichnus* is common in Paleozoic–Mesozoic fine-grained marine deposits, and is considered by some authors a poorly preserved *Chondrites*. Moreover, its

Table 1 Classification of the recorded ichnotaxa from the Cenomanian–Turonian succession of the Khanguet Grouz section

Ichnotaxa	Ethological category	Pre-/post-depositional	Toponomy	Abundance	Possible tracemakers	References
Chondrites isp.	Fodinichnia, Agrichnia, Chemichnia	Post	Endichnia	Common	Worm-like organisms, bivalves	Bromley and Ekdale (1984); Baucon et al. (2020)
Pilichnus isp.	Chemichnia, Fodinichnia	Post	Epichnia	Rare	Vermiform animals	Mikuláš (1997); Mángano and Buatois (2016)
Planolites isp.	Fodinichnia, Pascichnia	Post	Epichnia, Hypichnia, Endichnia	Abundant	Polychaetes, bivalves, arthropods	Uchman (1995); Knaust (2017); Rodríguez-Tovar et al. (2020)
Ptychoplasma isp.	Repichnia	Post	Hypichnia	Common	Bivalves	Rindsberg (1994); Uchman et al. (2011)
?Thalassinoides isp.	Domichnia, Fodinichnia, Agrichnia	Post	Epichnia	Common	Decapod Crustaceans	Frey et al. (1984); Ekdale (1992); Myrow (1995); Bromley (1996)
?Trichichnus isp.	Domichnia	Post	Epichnia	Rare	Crustaceans, worm-like organisms	Frey (1970); Uchman (1995, 1999)

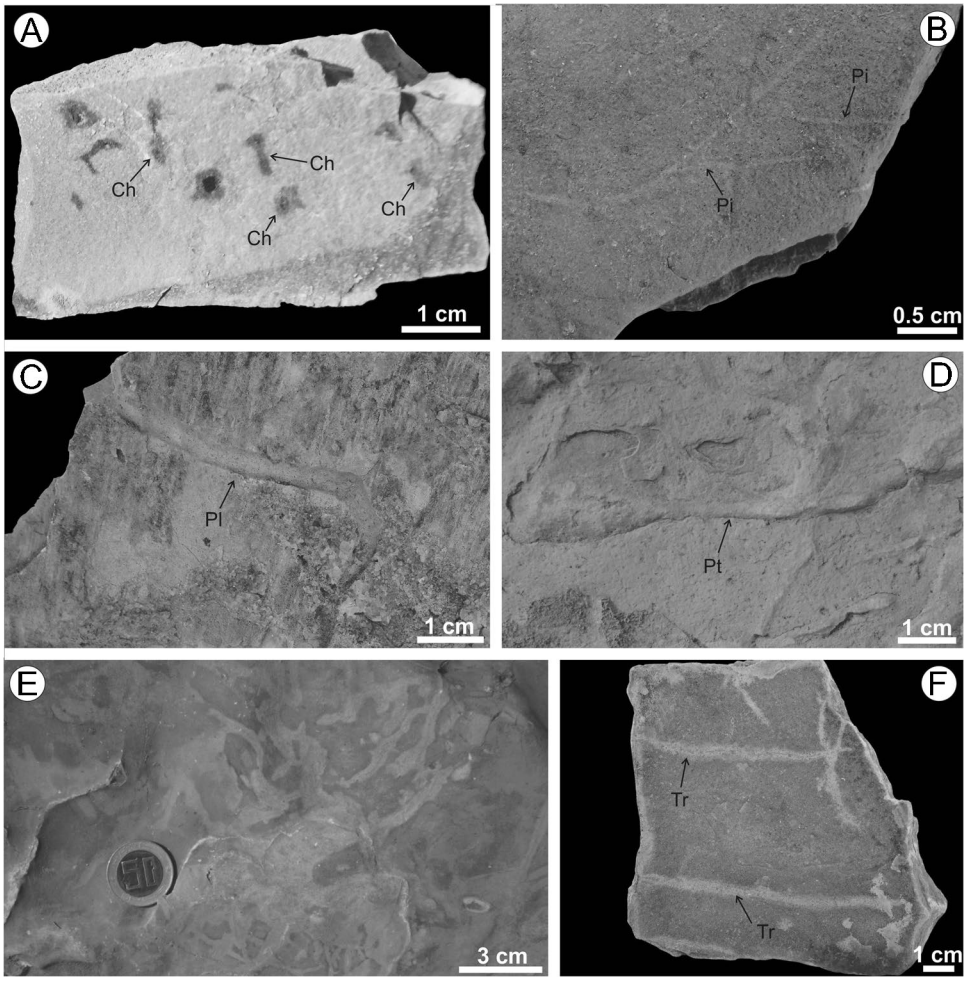

Fig. 4 Trace fossils of the Khanguet Grouz section. A *Chondrites* isp. B *Pilichnus* isp. C *Planolites* isp. D *Ptychoplasma* isp. E *?Thalassinoides* isp. F *?Trichichnus* isp

tracemaker preferred conditions that are also stressful for the rest of the infauna (Mikuláš et al. 2012). The latter is similar to the *Chondrites* producer. This trace fossil is considered a chemichnion, developed to absorb methane and hydrogen sulphide from the sediment (Mikuláš 1997; Mikuláš et al. 2012). It is regarded also as feeding structures of deposit feeders (Mángano and Buatois 2016), produced in very shallow tier by infaunal vermiform animals (Buatois and Mángano 2016). The studied specimens are the first recorded *Pilichnus* burrows from Algeria.

Planolites isp. (Fig. 4C)

The studied *Planolites* specimens consist of simple, horizontal, un-walled, unbranched straight or slightly curved burrows, preserved as epichnia, hypichnia and endichnia, and oriented more or less parallel to the bedding plane. They display a cylindrical to sub-cylindrical shape, and are filled sometimes by a purplish material. *Planolites* isp. specimens are 4-mm wide and up to 70-mm long. This trace fossil is found solitary or in association with *Chondrites* isp., *Ptychoplasma* isp. and *?Trichichnus* isp. The ichnogenus *Planolites* is a feeding (fodinichnion) trace fossil, produced by polychaetes and other worm-like deposit feeders, bivalves and arthropods, and it is known from the Ediacaran to the Holocene (e.g. Uchman 1995; Knaust 2017; Belaid et al. 2020; Naimi and Cherif 2021). These facies-crossing, actively filled burrows are also considered a pascichnion (e.g. Rodríguez-Tovar et al. 2020). It occurs in soft grounds from different aquatic environments (e.g. Uchman 1995). On continental shelf, the ichnogenus *Planolites* characterises the *Cruziana* ichnofacies (Buatois and Mángano 2011).

Ptychoplasma isp. (Fig. 4D)

Hypichnial, horizontal, slightly meandering, continuous ridges, 2–9-mm wide and 90-mm long, composed of uniserial, elongate, amygdaloidal to carinate mounds. This trace fossil co-occurs with *Planolites* isp. The ichnogenus *Ptychoplasma* is considered a repichnion mainly produced by bivalves; however, the amygdaloid mounds reflect resting periods in the life of a bivalve on the move (Rindsberg 1994; Uchman et al. 2011). This trace fossil is interpreted as the result of bivalve locomotion in the mud using a non-cleft

Table 2 Comparison of the C/TBE trace fossils (preceding, during and following theOAE-2) from different sections of the Tethyan realm. (1) Bottaccione section, Italy (Monaco et al. 2012, 2016); (2) Contessa section, Italy (Monaco et al. 2012, 2016); (3) Vergons section, France (Olivero and Gaillard 1996); (4) El Chorro section, Spain (Rodríguez-Tovar et al. 2009a); (5) Hedionda section, Spain (Rodríguez-Tovar et al. 2009a, b); (6) Rio Fardes, Spain (Rodríguez-Tovar et al.2020); (7) Barnasiówka, section A, Poland (Uchman et al.2008); (8) Barnasiówka, section B, Poland (Uchman et al.2008); (9) Sztolnia section, Poland (Uchman et al. 2013a); (10) Rybie section, Poland (Uchman et al. 2013b); (11) Trawne Stream section, Poland (Bąk et al. 2000); (12) Khanguet Grouz section, Algeria (present study)

	1	2	3	4	5	6	7	8	9	10	11	12
Alcyonidiopsis						×				×		
Chondrites	×	×	×	×	×	×	×	×	×	×	×	×
Halimedides									×			
Helicoraphe											×	
Lorenzinia											×	
Palaeophycus					×		×		×	×		
Pilichnus						×						×
Planolites	×	×		×	×	×	×	×	×	×	×	×
Protopaleodictyon											×	
Ptychoplasma												×
Scolicia											×	
Taenidium							×		×	×		
Thalassinoides	×	×		×	×	×	×	×	×	×		×
Teichichnus			×						×			
Trichichnus	×	×		×	×	×	×		×			×
Urohelminthoida											×	
Zoophycos	×	×		×	×				×	×	×	

wedge foot or a cleft foot (Uchman et al. 2011; Bhosle et al. 2019). The ichnogenus *Ptychoplasma* is known in marginal marine, shallow marine to deep-sea settings (Rindsberg 1994; Uchman et al. 2011; Cherif and Naimi 2022) and continental alluvial (crevasse splay) deposits (Pieńkowski and Uchman 2009). In the latter case, it reflects a repetitive rhythmic movement of the producing bivalves in accordance with the direction of flow (Pieńkowski and Uchman 2009).

?Thalassinoides isp. (Fig. 4E)

This ichnogenus addresses systems of burrows consisting of epichnial, horizontal, irregularly branched burrows, showing *Y*-shape and filled with a lighter and finer material than that of the host rock. *?Thalassinoides* isp. burrows are 5–10-mm wide and up to 90-mm long. *Thalassinoides* is a facies-crossing trace fossil, occurring in a wide range of environments (Myrow 1995; Kim et al. 2002), known from the Cambrian to the Holocene (e.g. Zhang et al. 2017; Bayet-Goll et al. 2021), with a single record in the Cambrian (Mikuláš 2000). It is considered a passively filled, domichnial trace fossil (Myrow 1995; Buatois et al. 2002), a fodinichnion (Ekdale 1992; Bromley 1996) and an agrichnion (Bromley 1996; Ekdale and Bromley 2003). This trace fossil is produced by decapod crustaceans (Frey et al. 1984). The ichnogenus *Thalassinoides* occurs in fine-grained, soft but cohesive sediments, characterising the shelf *Cruziana* ichnofacies and well-oxygenated conditions (e.g. Rodríguez-Tovar et al. 2020; Naimi and Cherif 2021). *Thalassinoides* ichnospecies can be found also in firmgrounds, but rarely in hardgrounds (Knaust 2017; Bayet-Goll et al. 2018). Within shallow marine settings, they indicate well-oxygenated water above the sea floor (e.g. Naimi et al. 2020).

?Trichichnus isp. (Fig. 4F)

They consist of poorly preserved, horizontal, thin, sometimes pyritised cylinders, which are 0.2-mm wide and 65–80-mm long. A rusty yellowish halo is present around the cylinders. These pyritised specimens of *?Trichichnus* isp. are whitish, occurring within a reddish oxidised facies, whereas the other specimens are purplish within whitish fine limestones. The latter are associated with *Chondrites* isp. and *Planolites* isp. The studied specimens are considered to constitute the first record from Algeria. The ichnogenus *Trichichnus* is a eurybathic trace fossil, characteristic of fine-grained shallow to deep marine deposits (Frey 1970; Wetzel 1983; Fillion and Pickerill 1990). Its filling displays a strong tendency toward pyritisation (Werner and Wetzel 1982; McBride and Picard 1991). It is regarded as dwelling structures of marine meiofaunal deposit feeders, such as crustaceans and worm-like organisms (Frey 1970). Later, Uchman (1995, 1999) linked this trace fossil to chemosymbiotic feeding, as in the case of the *Chondrites* tracemakers (Seilacher 1990; Fu 1991).

However, the ichnogenus *Trichichnus* occurs more deeply in sediments that are considered very poorly oxygenated, so it indicates a more opportunistic character than *Chondrites* (McBride and Picard 1991). Moreover, this trace fossil was considered fossilised filaments of sulphur bacteria living in the transition zone between anoxic and dysoxic sediments (Kędzierski et al. 2014).

Discussion

Palaeoenvironmental interpretation

The Upper Cenomanian–Lower Turonian interval of the Algerian Saharan Atlas, from the Ksour Range to the Ouled Nail Range, is characterised by carbonate platform deposits (Bassoullet 1973; Grosheny et al. 2008; Benyoucef et al. 2017; Benadla et al. 2018). These deposits are highly fossiliferous and carbonate-dominated due to the environmental change related to the major sea-level transgression (Benyoucef et al. 2017). The unit 1 of the studied section is characterised by sedimentologic, faunal and ichnologic contents which suggest a shallow marine setting as a depositional environment.

The lower part of the unit 2 was deposited within a marginal-marine environment. It shows many Lofer cyclothems. The latter are composed of three members: (i) Member C is composed of micritic limestones marked by a zone of intense stylolite development. These bed-parallel stylolites (diagenetic stylolites) appear to be developed in the fine-grained parts (micrite-rich horizons). They are due to layer-normal compression during burial and compaction, and play a key role in the dolomitisation and the subsequent hydrothermal corrosion affecting the carbonate platform deposits (Martín-Martín et al. 2018). Also, stylolites of shallow water carbonates may be formed during post-rift progressive subsidence of tectonic origin (Bertotti et al. 2017). Similar limestones from the Upper Albian of the Djebel Azzeddine section, located further to the north-east, were deposited in middle shoreface environment with well-oxygenated water above the sea floor (Naimi and Cherif 2021); (ii) member B is composed of stromatolitic limestones with tidal flat features such as tepee structures. They are characterised by small-scale growth faults (syn-depositional extensional faults), which are related to the subsidence in the coastal and continental shelf areas (Doglioni et al. 1998), and demonstrate a restricted intertidal zone; (iii) member A is represented by red palaeosols and loferitic breccia (supratidal soil conglomerates), considered diagnostic of a subaerial exposure related to pedogenetic process in nearby emerged areas, under dry and semi-arid conditions.

The upper part of unit 2 is represented by uppermost Cenomanian bioturbated dolomitic limestones (unit 2a = white mudstone bed sensu Grosheny et al. 2008), which yield the beginning of the $\delta^{13}C$ anomaly, and can be correlated with the Pre-Bahloul unit. They constitute the lower part of the Cenomanian–Turonian Bahloul Formation, evidenced in Tunisia (e.g. Amédro et al. 2005). These dolomitic limestones have also been correlated with the bed 63 of the C-T stratotype and section point at Pueblo, Colorado (Grosheny et al. 2008). This bed marks the beginning of the huge C/TB transgression (Grosheny et al. 2008). This transgression and its related deposits were evidenced in other regions from Algeria, such as the Tinrhert basin (Grosheny et al. 2013). In the Ksour Range, which occupy the western part of the Saharan Atlas basin, the base of the Rhoundjaïa Formation was interpreted as a transgressive surface (Benyoucef et al. 2017). The latter is marked by a lithological change, with peritidal stromatolite limestones passing into mid-ramp pseudo-nodular limestones. According to Grosheny et al. (2008), the $\delta^{13}C$ shift of the C/TBE coincides with the beginning of a transgressive trend accompanied by some gentle tectonic deformations of the northern Saharan margin. This tectonic activity is indicated in the Khanguet Grouz section by the presence of syn-sedimentary faults and stylolites, recorded in the shallow marine limestones of the unit 2 attributed to the Upper Cenomanian.

The overlying deposits of the unit 3 are characterised by lagoonal and marginal to shallow marine deposits displaying abundant stromatolites, Lofer cyclothems and chert beds (and thin levels). Some storm events were evidenced thanks to the presence of hummocky-cross stratifications. A lithological change, with peritidal algal limestones and Lofer cyclothems passing into micritic limestones and fine laminated shales indicating a deepening, marks the transition between units 3 and 4. The latter was deposited in an outer carbonate platform as indicated by the presence of the ostracods *Ovocytheridea producta*, *Brachycythere ekpo*, *Protobuntonia numidica* and *Bradleya* sp. (Herkat 1999). Their upper part is assigned to the Turonian based on inoceramid bivalves and ammonites (Grosheny et al. 2008; this work). Thereby, the Turonian ostracofauna of the Khanguet Grouz section suggests a shallower environment than that of the Aures basin, where black shales of the C/TBE were also deposited (Grosheny et al. 2008). The Lower Turonian offshore storm beds of Khanguet Grouz (Fig. 3N) pass laterally into rudist-bearing limestones in the Djebel Mimouna section located further to the south-east (Grosheny et al. 2008, 2013). The underlying Upper Cenomanian strata can also be correlated with the rudist biostromes we discovered recently in the Djebel Ousigna section. The latter are dominated by small clusters of *Caprinula* sp. and *Caprinula boissyi*. Another rudist-bearing level discovered by Emberger (1960) in this section is composed by isolated individuals of *Praeradiolites biskraensis* in life position. The latter are

intercalated within a lagoonal gypsum series, which constitutes the inner part of the carbonate platform.

In the Upper Cenomanian deposits of the Khanguet Grouz, the illite and illite-montmorillonite contents are 35% at the base of the succession; however, the illite content tends to be higher in the uppermost Cenomanian (Herkat 1999). The Turonian strata which correspond to a transgressive interval are characterised by the predominance of kaolinite (40%) and illite (40%) in their lower part. The clays of the middle part are dominated by montmorillonite (85%), illite (20%) and kaolinite (15%). Finally, their upper part shows essentially montmorillonite (60%), which is associated with illite and kaolinite with the same content (20% and 15%, respectively) (Herkat 1999). Hence, illite–smectite (usually montmorillonite) may be used as a geo-thermometer for mudrocks (Chamley 1989). This suggests that the Upper Cenomanian and the lowermost Turonian are characterised by a cold climate (Herkat 1999). Similar conditions were recognised at the C/TB of the Aquitaine basin in France, indicating climatic event attributed to cooling, accompanied with a replacement of Tethyan fauna by Boreal fauna (Moreau 1991; Herkat 1999). On the other hand, the clay content of the overlying Turonian strata indicates that the latter were deposited in a warm climate.

The black shales of the Khanguet Grouz section, as well as of other sections from Tunisia and eastern Algeria, were deposited continuously in corridors through the upper most Cenomanian and the Lower Turonian (*Mammites nodosoides* ammonite zone) (Grosheny et al. 2013). According to these authors, the carbonate platforms were flooded during the second part of the $\delta^{13}C$ shift.

The unit 5 was deposited in a shallow marine carbonate platform, characterised by many storm events and repeated emersion as indicated by the tepee structures and the evaporite-dissolution breccias (Grosheny et al. 2008).

Stable carbon isotope ($\delta.^{13}C$) interpretation and regional correlation

In general, the stable carbon isotope in carbonate rocks is very helpful in Cretaceous successions for the (i) changes in the mass balance of the global carbon cycle (Bachan et al. 2017); (ii) for regional and global correlation (Tsikos et al. 2005); and (iii) as a chemostratigraphic tool (Wendler 2013). The Cenomanian–Turonian boundary event (C/TBE) is well-known worldwide as the Oceanic Anoxic Event 2 with high concentrations of organic matter. Many stratigraphic studies of carbonate carbon isotopes have been carried in the western part of Algeria (Ksour Mountains), in its eastern part (Tebessa region) and finally in the Algerian-Tunisian border (Tunisian Atlas) (e.g. Amédro et al. 2005; Salmi-Laouar et al. 2018; Salhi et al. 2020). The investigation of stable carbon isotope in our study area allows showing three different events and comparing with other regional area. The first event is recorded in the unit 3 at 56 m ($\delta^{13}C_{carb} = 4.2$ ‰) and represents by micritic limestones with rare fauna. This event was formerly documented during Upper Cenomanian in Ksour Mountains at *Metoicoceras geslinianum* Zone (Salhi et al. 2020), in Tebessa at *Rotalipora cushmani* Zone (Salmi-Laouar et al. 2018) and in western Tunisia at *Metoicoceras geslinianum* Zone (Amédro et al. 2005). This first positive value coincides with the Upper Cenomanian transgression.

The second event is recorded in the lower part of unit 4 at 64 m ($\delta^{13}C_{carb} = 3.3$ ‰) and represents the apparition of filaments. This event was formerly documented in the Upper Cenomanian–Lower Turonian transition in Ksour Mountains (Salhi et al. 2020) at the transition from *Gamai* to *Cauvini* Zones, in Tebessa at the top of *Watinoceras* Zone and the first occurrence of *W. praehelvetica* (Salmi-Laouar et al. 2018), and in western Tunisia at the lower base of *Watinoceras* Zone (Amédro et al. 2005). This second positive value indicates the Upper Cenomanian–Lower Turonian boundary.

The third event is recorded in most of unit 4 and marked by a perturbation of $\delta^{13}C_{carb}$ ranging between −0.3 and +3.1 ‰, and it is represented by laminated white and black shales. This event was formerly documented in the Lower to Middle Turonian in Ksour Mountains and marked by a fluctuation of negative values (Salhi et al. 2020), in Tebessa by a fluctuation of positive values at the *Pseudospidoceras flexuosum* Zone (Salmi-Laouar et al. 2018), in western Tunisia also by a fluctuation of positive values at the *P. flexuosum* event (Amédro et al. 2005). We suggest that this perturbation of $\delta^{13}C$ values is linked to the degradation of organic matter under dysoxic environment or by changes in paleo-environmental conditions, salinity and/or temperature (Salmi-Laouar et al. 2018).

Vertical evolution of trace fossils

The pre-event interval (units 1 and 2) is characterised by ichnoassemblages dominated by horizontal burrows attributed to *Planolites* and *Ptychoplasma*. Other undetermined ichnofossils are present. In this interval, there is a high degree of bioturbation (BI = 4 to 5). These trace fossils indicate that the ecological niche was occupied by different organisms and represent variable ethology, such as repichnia, fodinichnia and/or pascichnia. These favourable conditions of macrobenthonic conditions are corroborated by the presence of bivalve and gastropod shells. Both trace fossils and body fossils suggest a shallow tier. The lithofacies indicate a marginal to shallow marine environment characterised by a high development of stromatolites and rare storm events corroborated by the presence of an oyster-rich limestone storm bed, in which, the shells are fragmented and randomly oriented.

The first part of the black shale (or OAE-2) interval (sensu Grosheny et al. 2008) corresponds to unit 3. It is characterised by an important change in ichnological features as revealed by the decrease of trace fossils. The most important part of the recorded traces has not been identified, while some burrows were attributed to *?Thalassinoides*. The ichnogenus *Planolites*, which constitutes the most common ichnotaxa from the studied section, is absent in this unit. The overlying greyish micritic limestones constituting the base of the unit 4 are marked by a generalised scarcity (BI = 1) or even a total absence (BI = 0) of trace fossils. Thus, only three ichnotaxa were recorded: *Planolites* isp., *Pilichnus* isp. and *?Trichichnus* isp. *Pilichnus* burrows indicate stressful conditions such as a lack of oxygen near the bottom and in the sediment, and relatively deeply buried or already partly lithified substrates (Mikuláš et al. 2012). Moreover, *Trichichnus* tracemakers have a higher tolerance for dysoxia than those of *Chondrites* (McBride and Picard 1991). The stressful conditions in this part of the section can be confirmed by the presence of dwarf forms of bivalves which were found in the whitish shales intercalated between the greyish, micritic limestone beds (Fig. 3I). The latter are overlain by thick shales. In their lower part, *Planolites* and *?Trichichnus* are associated with *Chondrites*. *Chondrites* tracemakers may prefer real extreme ecological situations (Wetzel and Uchman 2001). They have been interpreted as deposit feeders (Simpson 1957), users of chemosymbionts (Seilacher 1990; Fu 1991) and grazers of surface sediments (Kotake 1991). Also, the producers of this trace fossil occur in layers barren in organic matter (Kotake 1991). They may be present in oxygen-deficient deposits during de-oxygenation and re-oxygenation (e.g. Seilacher 1978; Bromley and Ekdale 1984; Savrda and Bottjer 1986; Wetzel and Uchman 2001). Furthermore, *Chondrites* tracemakers reworked a more confined volume than the producers of other trace fossils such as *Nereites* and *Phycosiphon* (Wetzel and Uchman 2001). These authors indicated that, in a shallow marine position, the strategy of the *Chondrites* producer may represent colonisation. The black shales of the middle part of unit 4 are unburrowed to sparsely burrowed. Thereby, the more characteristic trace fossil of stressful conditions, i.e. the ichnogenus *Chondrites*, occurs sparsely in dark muds (Martin and Pollard 1996). The alternation of whitish shales containing *Chondrites*, *Planolites* and *?Trichichnus*, with black shales characterised by primary horizontal laminations in the middle part of unit 4, indicates episodes of improved paleoenvironmental conditions during which *Chondrites*, *Pilichnus* and *?Trichichnus* producers could colonise the substrate in unfavourable and dysoxic to anoxic benthonic conditions. Short alternating oxic conditions may be indicated by the presence of levels which yielded benthic fauna such as inoceramid bivalves. The remaining part of unit 4 is characterised by abundant *Planolites* and other undetermined burrows, with the presence of high bioturbated levels (BI = 4 to 5). This part can be interpreted as a recovery phase (post-event phase), although Grosheny et al. (2008) considered them as part of the black shales.

The ichnologic record of the C/TBE from the Betic Cordillera in Spain (Rodríguez-Tovar et al. 2009a, b, 2020), the Apennines in Italy (Monaco et al. 2012, 2016) and the Outer Carpathians in Poland (Uchman et al. 2008, 2013a, b) is characterised by an important decrease in ichnoabundance and ichnodiversity, due to a significant decrease in the oxygenation of pore water. However, some fluctuations in this ichnologic record reveal the presence of short-time improvement to dysoxic or oxic conditions. The same conditions are evidenced in the Khanguet Grouz section, especially in the middle part of unit 4, where black shales occur. From an ichnologic point of view, dysoxic conditions interrupted by short intervals of anoxia were recorded in unit 4, between the upper part of the greyish micritic limestones and the lower part of the whitish shales (69–79 m). Accordingly, this part of the section should contain the Bonarelli Level.

Ichnology of the C/TB in the Tethyan realm

In the northern part of the Tethyan realm, trace fossils and ichnofabrics were used to determine the paleoecology, paleobiology and oxygenation change during the C/TBE. In this study, the trace fossils at hand are compared with those of 11 other sections from the northern Tethyan margin (Table 2): the Bottaccione and the Contessa sections from the Italian Apennines (Monaco et al. 2012, 2016); the Vergons section from the French Alps (Olivero and Gaillard 1996); the El Chorro, Hedionda and the Rio Fardes sections from the Spanish Betic Cordillera (Rodríguez-Tovar et al. 2009a, b, 2020); and the Barnasiówka, Rybie, Sztolnia and Trawne Stream sections from the Polish Outer Carpathians (Bąk et al. 2000; Uchman et al. 2008, 2013a, b).

The trace fossil *Chondrites* appears in all the other 11 Sects. (100%), *Pilichnus* in 1 Sect. (9.09%), *Planolites* in 10 Sects. (90.9%), *Ptychoplasma* has never been reported from pre-Bonarelli levels (0%), *Thalassinoides* is present in 9 Sects. (81.81%) and finally *Trichichnus* is reported in 7 Sects. (63.63%). Thereby, the five ichnotaxa *Chondrites*, *Planolites*, *Thalassinoides*, *Trichichnus* and *Zoophycos* are the most characteristic traces of the C/TBE (see Table 2). The absence of *Zoophycos* in the Khanguet Grouz section is due to environmental conditions. On the other hand, the presence of the four other ichnogenera led us to consider the investigated ichnoassemblage as typical forms of the OAE-2 related deposits in the Tethyan realm.

If we exclude the pre-OAE-2 levels, the most similar ichnoassemblage shown in Table 2 is that of the Rio Fardes section with 5 ichnogenera (100%) (Rodríguez-Tovar et al. 2020). Four ichnotaxa (*Chondrites*, *Planolites*,

Thalassinoides and *Trichichnus*) among the five (80%) recorded in the C/TBE deposits of the Khanguet Grouz section were reported from the C/TBE deposits of the Bottaccione, Contessa, El Chorro, Hedionda, Barnasiówka (A) and Sztolnia sections (Uchman et al. 2008, 2013a; Rodríguez-Tovar et al. 2009a, b; Monaco et al. 2012, 2016). In the Rybie section, both *Pilichnus* and *Trichichnus* are absent (Uchman et al. 2013b). Another trace fossil reported from the C/TBE deposits is *Teichichnus*. The latter has been found only in two sections, in Vergons (Olivero and Gaillard 1996), and Sztolnia (Uchman et al. 2013a). The latter is characterised by a lower thickness and number of anoxic layers, in comparison with the Spanish sections.

Conclusions

The Cenomanian–Turonian succession of the Khanguet Grouz section (Ouled Nail Range, Algerian Saharan Atlas) had been investigated based on their ichnologic, sedimentological and faunal contents, in order to provide new insights on the palaeoenvironment and the response of the endobenthic tracemaker community to the C/TBE.

Six trace fossils are found: *Chondrites* isp., *Pilichnus* isp., *Planolites* isp., *Ptychoplasma* isp., *?Thalassinoides* isp. and *?Trichichnus* isp. The pre-event deposits are characterised ichnoassemblages dominated by the ichnofossils *Planolites* and *Ptychoplasma*, and by a high degree of bioturbation. This indicates that different organisms, of variable ethology, occupied the ecological niche before the OAE-2. The decrease or the total absence of trace fossils in the sediments related to the C/TBE indicates an important change in environmental conditions. The recorded traces from these deposits are *Chondrites*, *Pilichnus*, *Planolites*, *?Thalassinoides* and *?Trichichnus*. They indicate stressful conditions. The presence of dwarf forms of bivalves confirms these latter. Black shales are present in the middle part of unit 4. They are laminated and unbioturbated. This indicates episodes of improved palaeoenvironmental conditions during which *Chondrites*, *Pilichnus* and *?Trichichnus* producers had colonised the substrate in unfavourable and dysoxic to anoxic benthic conditions. On the other hand, short alternating oxic conditions may be indicated by the presence of levels which yielded inoceramid bivalves. The recovery phase is characterised by *Planolites*, with strongly bioturbated levels. The trace fossil assemblage of the Khanguet Grouz section is more or less similar to the ichnoassemblages recorded from the northern Tethyan margin in Spain, Poland, Italy and France.

Other studies on the foraminiferal biostratigraphy of the C/TB interval are required in the Khanguet Grouz section, in order to establish a high-resolution ichnologic analysis of the coeval 'Bonarelli Level'.

Acknowledgements We thank also the journal reviewers Aram Bayet-Goll (Zanjan, Iran) and an anonymous reviewer, as well as the journal editor Abdullah M. Al-Amri and associated editor Aitor Payros for helpful comments and constructive criticism that greatly improved the manuscript. We gratefully thank Alfred Uchman (Jagiellonian, Poland) for fruitful discussions on the ichnotaxonomic affinities of the studied traces. Tuna Eren (Ankara, Turkey) is particularly thanked for the linguistic revision of the paper.

Declarations

Conflict of interest The authors declare no competing interests.

References

Amédro F, Accarie H, Robaszynski F (2005) Position de la limite Cénomanien-Turonien dans la Formation Bahloul de Tunisia centrale: apports intégrés des ammonites et des isotopes du carbone ($\delta^{13}C$). Eclogae Geol Helv 98:151–167

Arthur MA, Dean WE, Pratt LM (1988) Geochemical and climatic effects of increased marine organic carbon burial at the Cenomanian-Turonian boundary. Nature 335:714–717

Bachan A, Lau KV, Saltzman MR, Thomas E, Kump LR, Payne JL (2017) A model for the decrease in amplitude of carbon isotope excursions across the Phanerozoic. Am J Sci 317(6):641–676

Bąk K, Uchman A, Bąk M (2000) Agglutinated foraminifera, radiolaria and trace fossils from Upper Cretaceous deep-water variegated shales at Trawne Stream, Grajcarek Unit, Pieniny Klippen Belt, Carpathians, Poland. Bull Polish Acad Sci, Earth Sci 48:1–32

Bassoullet JP (1973) Contribution à l'étude stratigraphique du Mésozoïque de l'Atlas Saharien occidental (Algérie). Thèse de Doctorat Ès-Sciences, Université de Paris VI, pp 497

Bayet-Goll A, de Carvalho CN, Moussavi-Harami R, Mahboubi A, Nasiri Y (2014) Depositional environments and ichnology of the deep-marine succession of the Amiran Formation (upper Maastrichtian–Paleocene), Lurestan Province, Zagros Fold-Thrust Belt, Iran. Palaeogeogr, Palaeoclimatol, Palaeoecol 401:13–42

Bayet-Goll A, Samani PN, de Carvalho CN, Monaco P, Khodaie N, Pour MM, Kazemeini H, Zareiyan MH (2017) Sequence stratigraphy and ichnology of Early Cretaceous reservoirs, Gadvan Formation in southwestern Iran. Mar Pet Geol 81:294–319

Bayet-Goll A, de Carvalho CN, Daraei M, Monaco P, Sharafi M (2018) Sequence stratigraphic and sedimentologic significance of the trace fossil *Rhizocorallium* in the Upper Triassic Nayband Formation, Tabas Block, Central Iran. Palaeogeogr Palaeoclimatol Palaeoecol 491:196–217

Bayet-Goll A, Daraei M, Taher SPM, Etemad-Saeed N, de Carvalho CN, Zandkarimi K, Monaco P, Zohdi A, Rabbani J, Nasiri Y (2020) Variations of the trace fossil *Zoophycos* with respect to paleoenvironment and sequence stratigraphy in the Mississippian Mobarak Formation, northern Iran. Palaeogeogr Palaeoclimatol Palaeoecol 551:109754

Bayet-Goll A, Daraei M, Geyer G, Bahrami N, Bagheri F (2021) Environmental constraints on the distribution of matground and mixground ecosystems across the Cambrian Series 2–Miaolingian boundary interval in Iran: a case study for central sector of northern Gondwana. J Afr Earth Sc 176:104120

Baucon A, Bednarz M, Dufour S, Felletti F, Malgesini G, de Carvalho CN, Niklas KJ, Wehrmann A, Batstone R, Bernardini F, Briguglio A, Cabella R, Cavalazzi B, Ferretti A, Zanzerl H, McIlroy D (2020) Ethology of the trace fossil *Chondrites*: form, function and environment. Earth Sci Rev 202:102989

Belaid M, Cherif A, Vinn O, Naimi MN (2020) First record of trace fossils from the Oxfordian Argiles rouges de Kheneg Formation (Tiaret, northwestern Algeria). Geologica Croatica 73:85–94

Benadla M, Reolid M, Marok A, El Kamali N (2018) The Cenomanian-Turonian transition in the carbonate platform facies of the Western Saharan Atlas (Rhoundjaïa Formation, Algeria). J Iber Geol 44:405–429

Benhamou M, Brahim M (2020) Gisement d'ichtyofaunes et faciès associés au passage Cénomanien-Turonien dans la région de l'Ouarsenis (Algérie du Nord): coupes de reference, correlation régionale et approche paléobiogéographique. Mémoire Du Service Géologique De L'algérie 21:103–126

Benyoucef M, Mebarki K, Ferré B, Adaci M, Bulot LG, Desmares D, Villier L, Bensalah M, Frau C, Ifrim C, Malti FZ (2017) Litho- and biostratigraphy, facies patterns and depositional sequences of the Cenomanian-Turonian deposits in the Ksour Mountains (Saharan Atlas, Algeria). Cretac Res 78:34–55

Bertotti G, de Graaf S, Bisdom K, Oskam B, Vonhof HB, Bezerra FHR, Reijmer JJG, Cazarin CL (2017) Fracturing and fluid-flow during post-rift subsidence in carbonates of the Jandaíra Formation, Potiguar Basin, NE Brazil. Basin Res 29:836–853

Bhosle B, Johnson C, Vaghela S, Schultz DJ, Dholakia V (2019) First report: trace fossil assemblage *Ptychoplasma* (*P. excelsum*, *P. vagans*), *Dendroidichnites* (*D. irregulare*), *Ctenopholeus (?C. kutcheri*) and *Bergaueria* (*B. hemispherica*) in the cretaceous rocks of Bagh Formation, Mainland Gujarat, India. Ichnos 26:256–265

Bromley RG (1996) Trace fossils, Biology, Taphonomy and Applications, 2nd edn. Chapman and Hall, London, p 361

Bromley RG, Ekdale AA (1984) *Chondrites*: a trace fossil indicator of anoxia in sediments. Science 224:872–874

Buatois LA, Mángano MG (2011) Ichnology: organism-substrate interactions in space and time, Cambridge University Press, p 358

Buatois LA, Mángano MG (2016) Recurrent patterns and processes: the significance of ichnology in evolutionary paleoecology. In: Mángano MG, Buatois LA (Eds.), The trace-fossil record of major evolutionary events. vol 2: Mesozoic and Cenozoic. Springer, pp 449–473

Buatois LA, Mángano MG, Aceñolaza F (2002) Trazas Fósiles. Señales de comportamiento en el Registro Estratigráfico. Museo Paleontológico Egidio Feruglio, Chubut, p 382

Chamley H (1989) Clay sedimentology. Springer-Verlag, Berlin Heidelberg, p 623

Cherif A, Naimi MN (2022) A diverse ichnofauna and its palaeoenvironmental significance from the Upper Jurassic Argiles de Saïda Formation (Northwestern Algeria). Hist Biol 34:624–647

Cherif A, Bert D, Benhamou M, Benyoucef M (2015) La Formation des Argiles de Saïda (Jurassique supérieur) dans le domaine tlemcenien oriental (Takhemaret, Algérie): données biostratigraphiques, ichnologiques et sédimentologiques. Rev Paléobiol 34:363–384

Cherif A, Benyoucef M, Naimi MN, Ferré B, Zeghari A, Frau C, Berrabah A (2021a) Trace fossils from the Berriasian-Valanginian of the Ouarsenis Range (northwestern Algeria) and their paleoenvironmental implications. J Afr Earth Sc 180:104219

Cherif A, Naimi MN, Belaid M (2021b) Deep-sea trace fossils and depositional model from the lower Miocene Tiaret Marl Formation (northwestern Algeria). J Afr Earth Sc 175:104115

Chikhi-Aouimeur F, Grosheny D, Ferry S, Herkat M, Jati M, Atrops F, Redjimi-Bourouiba W, Benkherouf-Kechid F (2011) Lithofaciès, paléogéographie et correlations au passage Cénomanien-Turonien dans l'Atlas Saharien (Ouled Naïl, Zibans, Aurès et Hodna, Algérie). Mémoires Du Service Géologique National 17:67–83

Djebbar T (2000) Structural evolution of the Algerian Saharan Atlas PhD thesis. Royal Holloway University of London, United Kingdom, p 373

Doglioni C, D'Agostino N, Mariotti G (1998) Normal faulting vs regional subsidence and sedimentation rate. Mar Pet Geol 15:737–750

Ekdale AA (1992) Muckraking and mudslinging: the joys of deposit-feeding. In: Maples CG, West RR (Eds.), Trace fossils: paleontological society, short courses in paleontology 5, 145–171

Ekdale AA, Bromley RG (2003) Paleoethologic interpretation of complex *Thalassinoides* in shallow-marine limestones, Lower Ordovician, southern Sweden. Palaeogeogr Palaeoclimatol Palaeoecol 192:221–227

Emberger J (1960) Esquisse géologique de la partie orientale des Monts des Ouled Naïl (Atlas saharien, Algérie). Publications Du Service De La Carte Géologique De L'algérie 27:1–398

Fillion D, Pickerill RK (1990) Ichnology of the Upper Cambrian? To Lower Ordovician Bell Island and Wabana groups of eastern Newfoundland, Canada. Palaeontogr Can 7:1–119

Frey RW (1970) Trace fossils of Fort Hays Limestone Member of Niobrara Chalk (Upper Cretaceous), west-central Kansas. Univ Kansas Paleonto Contrib 53:1–41

Frey RW, Curran AH, Pemberton GS (1984) Tracemaking activities of crabs and their environmental significance: the ichnogenus *Psilonichnus*. J Paleontol 58:511–528

Fu S (1991) Funktion, Verhalten und Einteilung fucoider und lophoctenoider Lebensspuren. Cour Forschungsinst Senck 135:1–79

Gradstein FM, Ogg JG, Schmitz MD, Ogg GM (2012) The geologic time scale 2012. Elsevier, Amsterdam

Grosheny D, Chikhi-Aouimeur F, Ferry S, Benkherouf-Kechid F, Jati M, Atrops F, Redjimi-Bourouiba W (2008) The Upper Cenomanian-Turonian (Upper Cretaceous) of the Saharan Atlas (Algeria). Bull De La Société Géologique De France 179:593–603

Grosheny D, Ferry S, Jati M, Ouaja M, Bensalah M, Atrops F, Chikhi-Aouimeur F, Benkherouf-Kechid F, Negra H, Aït Salem H (2013) The Cenomanian-Turonian boundary on the Saharan Platform (Tunisia and Algeria). Cretac Res 42:66–84

Guiraud R (1973) Evolution post-triasique de l'avant-pays de la chaîne en Algérie d'après l'étude du Bassin du Hodna et des regions voisines. Thèse de Doctorat Ès-Sciences, Université de Nice, France, p 270

Hallam A, Wignall PB (1997) Mass extinctions and their aftermath. Oxford University Press, Oxford

Haq BU, Hardenbol J, Vail PR (1987) Chronology of fluctuating sea levels since the Triassic. Science 235:1156–1166

Hart MB (1980) A water depth model for the evolution of the planktonic Foraminiferida. Nature 286:252–254

Hassani M, Chabou MC, Haddoum H, Hamoudi M (2016) Tectonic control on the morphology of the subcircular structure of El Medaouar (Saharan Atlas, Algeria): insights from geological and remote sensing data. Arab J Geosci 9:632

Herkat M (1999) La sedimentation de haut niveau marin du Crétacé supérieur de l'Atlas saharien oriental et des Aurès. Stratigraphie séquentielle, analyse quantitative des biocénoses, évolution paléogéographique et contexte géodynamique. Thèse de Doctorat Ès-Sciences, USTHB, Algiers, Algeria, p 802

Kazi-Tani N (1986) Evolution géodynamique de la bordure nord-africaine: le domaine intraplaque nord-algérien. Approche mégaséquentielle. Thèse de Doctorat Ès-Sciences, Université de Pau et des Pays de l'Adour, France, p 871

Kędzierski M, Uchman A, Sawlowicz Z, Briguglui A (2014) Fossilized bioelectric wire – the trace fossil *Trichichnus*. Biogeosci Discuss 11:17707–17728

Kennedy WJ, Walaszczyk I, Cobban WA (2000) Pueblo, Colorado, USA, candidate Global Boundary Stratotype Section and Point for the base of the Turonian Stage of the Cretaceous, and for the base of the Middle Turonian Substage, with a revision of the Inoceramidae (Bivalvia). Acta Geol Pol 50:295–334

Kennedy WJ, Walaszczyk I, Cobban WA (2005) The Global Boundary Stratotype Section and Point for the base of the Turonian stage of the Cretaceous: Pueblo, Colorado, U.S.A. Episodes 28:93–104

Kim JY, Kim KS, Pickerill RK (2002) Cretaceous nonmarine trace fossils from the Hasandong and Jinju Formations of the Namhae area, Kyongsangnamdo, Southeast Korea. Ichnos 9:41–60

Knaust D (2012a) Trace-fossil systematics. In: Knaust D, Bromley RG (Eds.), Trace fossils as indicators of sedimentary environments. Developments in Sedimentology, 64, Elsevier, pp 79–101

Knaust D (2012b) Methodology and techniques. In: Knaust D, Bromley RG (Eds.), Trace fossils as indicators of sedimentary environments. Developments in Sedimentology, 64, Elsevier, pp 245–271

Knaust D (2017) Atlas of trace fossils in well core: appearance, taxonomy and interpretation. Springer, p 209

Kotake N (1991) Packing process for the filling material in *Chondrites*. Ichnos 1:277–285

Łaska W, Rodríguez-Tovar FJ, Uchman A (2017) Evaluating macrobenthic response to the Cretaceous-Paleogene event: a high-resolution ichnological approach at the Agost section (SE Spain). Cretac Res 70:96–110

Leckie RM, Bralower TJ, Cashman R (2002) Oceanic anoxic events and plankton evolution: Biotic response to tectonic forcing during the mid-Cretaceous. Paleoceanography 17:1–29

Mángano MG, Buatois LA (2016) The Cambrian explosion. In: Mángano MG, Buatois LA (Eds.) The trace-fossil record of major evolutionary events. Vol 1: Precambrian and Paleozoic. Springer, pp 73–126

Martin M, Pollard J (1996) The role of trace fossil (ichnofabric) analysis in the development of depositional models for the Upper Jurassic Fulmar Formation of the Kittiwake Field (Quadrant 21 UKCS). In: Hurst A et al. (Eds.), Geology of the Humber Group: Central Graben and Moray Firth. Geological Society Special Publications, UKCS, 114: pp 163–183

Martín-Martín JD, Gomez-Rivas E, Gomez-Gras D, Travé A, Ameneiro R, Koehn D, Bons D (2018) Activation of stylolites as conduits for overpressured fluid flow in dolomitized platform carbonates. Geolo Soc, London, Spec Publ 459:157–176

Martinsson A (1970) Toponomy of trace fossils. In: Crimes TP, Harper JC (Eds.), Trace fossils. Geological Journal, Special issue 3: pp 323–330

McBride EF, Picard DM (1991) Facies implications of Trichichnus and Chondrites in turbidites and hemipelagites, Marnoso-arenacea Formation (Miocene), Northern Apennines, Italy. Palaios 6:281–290

Miguez-Salas O, Rodríguez-Tovar FJ, Duarte LV (2017) Selective incidence of the Toarcian Oceanic Anoxic Event (T-OAE) on macroinvertebrate marine communities: a case from the Lusitanian basin (Portugal). Lethaia 50:548–560

Mikuláš R (1997) Ethological interpretation of the ichnogenus *Pragichnus* Chulpáč, 1987 (Ordovician, Czech Republic). N Jb Geol Paläont 1997:93–108

Mikuláš R (2000) Trace fossils from the Cambrian of the Barrandianarea. Czech Geol Surv Spec Paper 12:1–29

Mikuláš R, Fatka O, Szabad M (2012) Paleoecologic implications of ichnofossils associated with slightly skeletonized body fossils, Middle Cambrian of the Barrandian Area, Czech Republic. Ichnos 19:199–210

Monaco P, Rodríguez-Tovar FJ, Uchman A (2012) Ichnological analysis of lateral environmental heterogeneity within the Bonarelli Level (uppermost Cenomanian) in the classical localities near Gubbio, Central Apennines, Italy. Palaios 27:48–54

Monaco P, Rodríguez-Tovar FJ, Uchman A (2016) Environmental fluctuations during the latest Cenomanian (Bonarelli Level) in the Gubbio area (central Italy) based on an ichnofabric approach. In: Menichetti M, Coccioni R, Montanari A (Eds.), The stratigraphic record of Gubbio: integrated stratigraphy of the Late Cretaceous–Paleogene Umbria-Marche Pelagic Basin, vol 524. Geological Society of America Special Paper, pp 97–103

Moreau P (1991) Morphologie du Jurassique et du Crétacé supérieurs en pays cognaçais (Charente). Justification Géologique. Norois 38:427–437

Myrow PM (1995) *Thalassinoides* and the enigma of early Paleozoic open-framework burrow systems. Palaios 10:58–74

Naimi MN, Cherif A (2021) Sedimentology and ichnology of the mid-Cretaceous succession of Ouled Nail Mounts (Eastern Saharan Atlas, Algeria). Geologia Croatica 74(3):209–223

Naimi MN, Mansour B, Cherif A, Chekkali MC, Benkhedda A, Belaid M (2020) Lithostratigraphie et paléoenvironnements des dépôts messiniens de la terminaison nord-orientale des monts des Ouled Ali (bassin du Bas Chélif, Algérie nord-occidentale). Rev Paléobiol 39:467–483

Naimi MN, Mahboubi CY, Cherif A (2021a) Lithostratigraphy and evolution of the Lower Cretaceous Basins, in Western Saharan Atlas, Algeria: a comment. J Afr Earth Sc 183:104304

Naimi MN, Vinn O, Cherif A, Benyoucef M (2021b) *Trypanites* and associated bivalve borings in an Upper Albian hardground from the Eastern Saharan Atlas (Algeria). Proc Geol Assoc 132(5):529–536

Nasiri Y, Bayet-Goll A, Mahboubi A, Moussavi-Harami R, Monaco P (2020) Paleoenvironmental control on trace fossils across a Mississippian carbonate ramp succession, Mobarak Formation, east of Central and Eastern Alborz, Iran. J Afr Earth Sci 165:103800

Olivero D, Gaillard C (1996) Ichnologie du passage Cénomanien-Turonien. Exemple de la coupe de Vergons (Alpes de Haute-Provence, SE France). Comptes Rendus De L'académie Des Sciences, Paris 322:1005–1012

Pieńkowski G, Uchman A (2009) *Ptychoplasma conica* isp. nov. – a new bivalve locomotion trace fossil from the Lower Jurassic (Hettangian) alluvial sediments of Sołtyków, Holy Cross Mountains, Poland. Geol Q 53:397–406

Rindsberg AK (1994) Ichnology of the Upper Mississippian Hartselle Sandstone of Alabama, with notes on other Carboniferous formations. Geol Surv Alabama Bull 158:1–107

Ritter E (1902) Le Djebel Amour et les Monts des Oulad-Nayl. Bulletin Du Service De La Carte Géologique De L'algérie 2:1–97

Rodríguez-Tovar FJ, Uchman A (2017) The Faraoni event (latest Hauterivian) in ichnological record: The Rio Argos section of southern Spain. Cretac Res 79:109–121

Rodríguez-Tovar FJ, Uchman A, Martín-Algarra A, O'Dogherty L (2009a) Nutrient spatial variation during intrabasinal upwelling at the Cenomanian-Turonian oceanic anoxic event in the westernmost Tethys: an ichnological and facies approach. Sed Geol 215:83–93

Rodríguez-Tovar FJ, Uchman A, Martín-Algarra A (2009b) Oceanic anoxic event at the Cenomanian-Turonian boundary interval (OAE-2): ichnological approach from the Betic Cordillera, southern Spain. Lethaia 42:407–417

Rodríguez-Tovar FJ, Uchman A, Alegret L, Molina E (2011) Impact of the Paleocene-Eocene Thermal Maximum on the macrobenthic community: ichnological record from the Zumaia section, northern Spain. Mar Geol 282:178–187

Rodríguez-Tovar FJ, Uchman A, Reolid M, Sánchez-Quiñónez CA (2020) Ichnological analysis of the Cenomanian-Turonian boundary interval in a collapsing slope setting: a case from the Rio Fardes section, southern Spain. Cretac Res 106:104262

Rodríguez-Tovar FJ, Dorador J, Zuchuat V, Planke S, Hammer Ø (2021) Response of macrobenthic trace maker community to the end-Permian mass extinction in Central Spitsbergen, Svalbard. Palaeogeogr, Palaeoclimatol, Palaeoecol. https://doi.org/10.1016/j.palaeo.2021.110637

Ruault-Djerrab M, Kechid-Benkherouf F (2011) Micropaleontological study (foraminifera, ostracods) and characterization of the paleoenvironment of middle Cretaceous deposits (Djebel Chemla area, north-eastern Algeria). Arab J Geosci 4:1289–1299

Ruault-Djerrab M, Ferré B, Kechid-Benkherouf F (2012) Etude micropaléontologique du Cénomano-Turonien dans la région de Tébessa (NE Algérie): implications paléoenvironnementales et recherche de l'empreinte de l'OAE2. Rev Paléobiol 31:127–144

Ruault-Djerrab M, Kechid-Benkherouf F, Djerrab A (2014) Données paléoenvironnementales sur le Vraconnien/Cénomanien de la région de Tébessa (Atlas saharien, nord-est Algérie). Caractérisation de l'OAE2. Annales De Paléontologie 100:343–359

Salhi A, Atrops F, Benhamou M (2020) Le passage cénomanien-turonien dans les Monts des Ksour (Atlas Saharien Occidental, Algérie): biostratigraphie, géochimie et milieux de depot. Estud Geol 76:e135

Salmi-Laouar S, Ferré B, Chaabane K, Laouar R, Boyce AJ, Fallick AE (2018) The oceanic anoxic event 2 at Es Souabaa (Tebessa, NE Algeria): bio-events and stable isotope study. Arab J Geosci 11:182

Savrda CE, Bottjer DJ (1986) Trace-fossil model for reconstruction of paleo-oxygenation in bottom waters. Geology 14:3–6

Schlanger SO, Jenkyns HC (1976) Cretaceous oceanic anoxic events: causes and consequences. Geol Mijnbouw 55:179–184

Scholle PA, Arthur MA (1980) Carbon isotope fluctuations in Cretaceous pelagic limestones: potential stratigraphic and petroleum exploration tool. AAPG Bull 64:67–87

Scotese CR (2014) Atlas of Late Cretaceous Maps, PALEOMAP Atlas for ArcGIS, volume 2, The Cretaceous, Maps 16 – 22, Mollweide projection, PALEOMAP project, Evanston, IL

Seilacher A (1978) Use of trace fossil assemblages for recognizing depositional environments. In: Basan PB (Ed.), Trace fossil concepts. Society of Economic Paleontologists and Mineralogists Short Course Notes, 5, Tulsa (Oklahoma), pp 185–201

Seilacher A (1990) Aberration in bivalve evolution related to photo- and chemo-symbiosis. Hist Biol 3:289–311

Sharafi M, Rodríguez-Tovar FJ, Janočko J, Bayet-Goll A, Mohammadi M, Khanehbad M (2022) Environmental significance of trace fossil assemblages in a tide-wave-dominated shallow-marine carbonate system (Lower Cretaceous), northern Neo-Tethys margin, Kopet-Dagh Basin, Iran. Int J Earth Sci 111:103–126

Simpson S (1957) On the trace fossil *Chondrites*. Q J Geol Soc Lond 112:475–500

Stachacz M, Uchman A, Rodríguez-Tovar FJ (2017) Ichnological record of the Frasnian-Famennian boundary interval: two examples from the Holy Cross Mts (Central Poland). Int J Earth Sci 106:157–170

Taylor AM, Goldring R (1993) Description and analysis of bioturbation and ichnofabric. Geol Soc, London, Spec Publ 150:141–148

Tchenar S, Ferré B, Adaci M, Zaoui D, Benyoucef M, Bensalah M, Kentri T (2020) Incidences de l'Evènement Anoxique Océnique II sur l'évolution des ostracodes des dépôts cénomano-turoniens du bassin de Tinrhert (SE Algérie). Carnets De Géologie 20:145–164

Tsikos H, Jenkyns HC, Walsworth-Bell B, Petrizzo MR, Forster A, Kolonic S, Erba E, Silva IP, Baas M, Wagner T, Sinninghe JS (2005) Carbon-isotope stratigraphy recorded by the Cenomanian-Turonian Oceanic Anoxic Event: correlation and implications based on three key localities. J Geol Soc 161:711–719

Uchman A (1995) Taxonomy and palaeoecology of flysch trace fossils: the Marnoso-arenacea Formation and associated facies (Miocene, Northern Apennines, Italy). Beringeria 15:3–115

Uchman A (1999) Ichnology of the Rhenodanubian Flysch (Lower Cretaceous–Eocene) in Austria and Germany. Beringeria 25:65–171

Uchman A, Mikuláš R, Houša V (2003) The trace fossil *Chondrites* in uppermost Jurassic–lower Cretaceous deep cavity fills from the western Carpathians (Czech Republic). Geol Carpath 54:181–187

Uchman A, Bąk K, Rodríguez-Tovar FJ (2008) Ichnological record of deep-sea palaeoenvironmental changes around the Oceanic Anoxic Event 2 (Cenomanian–Turonian boundary): an example from the Barnasiówka section, Polish Outer Carpathians. Palaeogeogr Palaeoclimatol Palaeoecol 262:61–71

Uchman A, Mikuláš R, Rindsberg AK (2011) Mollusc trace fossils *Ptychoplasma* Fenton and Fenton, 1937 and *Oravaichnium* Plička and Uhrová, 1990: their type material and ichnospecies. Geobios 44:387–397

Uchman A, Caruso C, Sonnino M (2012) Taxonomic review of *Chondrites affinis* (Sternberg, 1833) from Cretaceous-Neogene offshore–deep-sea Tethyan sediments and recommendation for its further use. Riv Ital Paleontol Stratigr 118:313–324

Uchman A, Rodríguez-Tovar FJ, Oszczypko N (2013a) Exceptionally favourable life conditions for macrobenthos during the Late Cenomanian OAE-2 event: ichnological record from the Bonarelli Level in the Grajcarek Unit, Polish Carpathians. Cretac Res 46:1–10

Uchman A, Rodríguez-Tovar FJ, Machaniec E, Kędzierski M (2013b) Ichnological characteristics of Late Cretaceous hemipelagic and pelagic sediments in a submarine high around the OAE-2 event: a case from the Rybie section, Polish Carpathians. Palaeogeogr Palaeoclimatol Palaeoecol 370:222–231

Wendler I (2013) A critical evaluation of carbon isotope stratigraphy and biostratigraphic implications for Late Cretaceous global correlation. Earth Sci Rev 126:116–146

Werner F, Wetzel W (1982) Interpretation of biogenic structures in oceanic sediments. Bulletin De L'institut De Géologie Du Bassin D'aquitaine 31:275–288

Wetzel A (1983) Biogenic structures in modern slope to deep-sea sediments in the Sulu Sea Basin (Philippines). Palaeogeogr Palaeoclimatol Palaeoecol 42:285–304

Wetzel A, Uchman A (2001) Sequential colonization of muddy turbidites in the Eocene Beloveža Formation, Poland. Palaeogeogr Palaeoclimatol Palaeoecol 168:171–186

Wilmsen M, Berensmeier M, Fürsich FT, Schlagintweit F, Hairapetian V, Pashazadeh B, Majidifard MR (2020) Mid-Cretaceous biostratigraphy (ammonites, inoceramid bivalves and foraminifers) at the eastern margin of the Anarak Metamorphic Complex (Central Iran). Cretac Res 110:104411

Wonders AAH (1980) Middle and Late Cretaceous planktonic foraminifera of the western Mediterranean area. Utrecht Micropaleontol Bull 24:1–157

Zhang LJ, Qi YA, Buatois LA, Mangano MG, Meng Y, Li D (2017) The impact of deep-tier burrow systems in sediment mixing and ecosystem engineering in early Cambrian carbonate setting. Sci Rep 7:45773